FERMILAB-CONF-07-605-E

The first results of the GammeV axion-like particles search experiment

Jonghee Yoo

(for GammeV collaboration)

Fermi National Accelerator Laboratory, PO Box 500
Batavia, IL 60510, USA
E-mail: yoo@fnal.gov

We report the first results of the GammeV experiment, a search for meV mass particles converted from photons. The experiment uses a strong external magnetic field to induce oscillations between incident photons from a pulsed laser and axion-like particles. A mirror is placed at a position within the magnetic field such that photons can not pass through the second part of the magnetic field. On the other hand, the weakly interacting axion-like particles can pass through beyond the mirror and may convert back into the photons. The regenerated photons then detected with a photomultiplier tube. The oscillation baseline of the apparatus is designed to vary, allowing probes of different values of particle mass. We find no excess of events above background. The two-photon couplings of possible new scalar (pseudoscalar) particles to be less than 3.2×10^{-7} GeV^{-1} (3.2×10^{-7} GeV^{-1}) in the limit of massless particles.

Keywords: Axion, photon, dark matter

1. Introduction

Modern cosmology indicates that 23% of the Universe consists of dark matter. There are no lack of dark matter candidate particles such as the LSP, LKP, axion, axino, and gravitino. Any stable neutral non-baryonic massive particles can be a dark matter candidate. The axion is a dark matter candidate within the Standard Model regime. The axion was originally suggested to solve the strong CP problem in QCD by breaking U(1)$_{PQ}$ symmetry.[1,2]

The axion-like interaction Lagrangian for a pseudoscalar particle is given by:

$$\mathcal{L}_{\rm int} = -\frac{g}{4}\phi F_{\mu\nu}\widetilde{F}^{\mu\nu} = g\phi(\vec{E}\cdot\vec{B}) \qquad (1)$$

while that for a scalar particle is:

$$\mathcal{L}_{\rm int} = -\frac{g}{4}\phi F_{\mu\nu}F^{\mu\nu} = g\phi(\vec{E}\cdot\vec{E} - \vec{B}\cdot\vec{B}). \quad (2)$$

Micro cavity experiment is currently the most sensitive experiment to detect the cosmogenic cold-dark matter axions. ADMX experiment may be able to detect the photons from the resonant conversion of the axion in the magnetic field permeated microwave cavity using an ultra-low-noise receiver. The earlier results using an 1 liter cavity and HFET amplifier consistent with absence of the axion-dark matter in the mass range of $m_a \simeq 10^{-4} \sim 10^{-6}$ eV and axion-photon coupling scale of $g_{\gamma aa} \simeq 10^{-13} \sim 10^{-15}$ GeV^{-1}.[3,4]

Couplings of light particles to photons are constrained by considering stellar cooling. Cosmological, astrophysical and nuclear physical constraints restrict the allowed axion mass ranges 10^{-6} eV $\leq m_a \leq 10^{-2}$ eV and 3 eV $\leq m_a \leq 20$ eV.[5,6]

Recent reports from the PVLAS photon oscillation experiment showed a positive signal which may be interpreted as an evidence of a coupling of axion-like particle to photons.[7] Any weakly interacting two photon vertex particles produced by an oscillation would have escaped through the cavity mirrors if they are sufficiently weakly coupled to matter. PVLAS was able to determine a relative attenuation of laser polarization components transverse to and parallel to the external magnetic field. Newer PVLAS results[8] included the measurements of non-zero polarization rotation with 532 nm photons, and non-zero ellipticity.

The PVLAS measurements gave a consistent picture of a scalar mass $m_\phi \sim 1.2$ meV and a two-photon coupling scale $g \sim 2.5 \times 10^{-6}$ GeV^{-1}. The region is not excluded by the earlier BFRT experiment.[9,10] However, the PVLAS signals could not be reproduced after the experimental apparatus was rebuilt in an effort to improve the detection.[11] The reasons for the negative results are not clearly explained. The BMV experiment recently searched for regenerated photons and excluded at 99.9% C.L. the pseudoscalar interpretation of PVLAS signal.[12]

The GammeV experiment is designed to probe the region in parameter space suggested by the PVLAS results. The experiment is similar to that originally suggested by van Bibber et.al.[13] A positive signal would provide an unambiguous evidence of oscillations of photons into new weakly interacting particles.[14]

2. Experiment Setup

Figure 1 shows schematics of the GammeV experiment setup. There are three major component of the experiment. The photon source (laser), external magnetic field (Tevatron magnet) and photon read out (PMT). A Continuum Surelite I-20 Nd:YAG laser is used as the light source. The laser emits vertically polarized 160 mJ, 532 nm pulses of 5 ns width with a rate of 20 Hz. The vertical mode is used to probe pseudo-scaler particle search. For a scaler particle search, a half wave plate is used to obtain horizontal polarization mode. The laser lights are sent through a vacuum tight warm bore inserted into a 6 m Tevatron superconducting dipole magnet. The magnet produces a 5 T vertical field uniform across the aperture of the $1\frac{7}{8}$". A mirror located in the warm bore reflect back the beam to a power meter in the laser box in order not to heat up the magnet core. The mirror, on the end of a long hollow stainless steel "plunger", is inserted into the warm bore. The mirror may be placed at various positions within the magnet. In this experiment we have used two positions of plunger (center 2.9 m and edge 1 m) to cover entire PVLAS parameter space.

The beam passing through the end of the plunger is a pure (pseudo-)scalar beam. These particles can then oscillate back into photons through the magnetic field region after the mirror. The regenerated photons then propagates $\sim$ 5 m into a dark PMT box. A Hamamatsu H7422P PMT module is used to read out the photons.

The axion-photon oscillation probability can be written in GammeV engineering unit as :

$$P_{\gamma\to\phi} = \frac{4B^2\omega^2}{M^2(\Delta m^2)^2}\sin^2\left(\frac{\Delta m^2 L}{4\omega}\right) \tag{3}$$

$$\approx \frac{4B^2\omega^2}{M^2 m_\phi^4}\sin^2\left(\frac{m_\phi^2 L}{4\omega}\right) \tag{4}$$

$$= 1.5\times10^{-11}\frac{(B/\text{Tesla})^2(\omega/\text{eV})^2}{(M/10^5\ \text{GeV})^2(m_\phi/10^{-3}\ \text{eV})^4} \times\sin^2\left(1.267\frac{(m_\phi/10^{-3}\ \text{eV})^2(L/\text{m})}{(\omega/\text{eV})}\right) \tag{5}$$

where B is the strength of the external magnetic field, ω is the inital photon energy, L is the magnetic oscillation baseline. $\Delta m^2 = m_\phi^2 - m_\gamma^2$, the mass-squared difference between the scalar mass and the effective photon mass. The phase advance of photons in the vacuum region may be modelled with an effective mass $m_\gamma^2 = -2\omega^2(n-1)$, where n is the index of

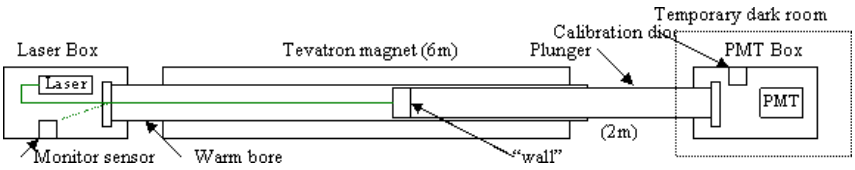

Fig. 1. Experiment setup of the GammeV.

refraction.[15] The warm bore and the interior of the plunger are pumped to vacuum pressures of 10^{-3} torr, and upper limit of the effective photon mass is estimated $\sqrt{-m_\gamma^2} < 4 \times 10^{-4}$ eV. The contribution from the effective photon mass is negligible the PVLAS allowed scaler mass region. The regeneration probability contains two factors of equation 4 and varies as $\sin^2\left(\frac{m_\phi^2 L_1}{4\omega}\right)\sin^2\left(\frac{m_\phi^2 L_2}{4\omega}\right)$ where $L_1 + L_2 = 6$ m.

The plunger guided into the PMT box and 2" lens to focus the beam onto the 5 mm diameter GaAsP photocathode of the PMT. The laser alignment is performed using a low power helium-neon laser. The alignment is verified before and after data-taking by replacing the sealed plunger with an open-ended plunger, and firing the Nd:YAG laser onto a flash paper target. An optical transport efficiency of 92% is measured using the ratio of laser power transmitted through the open-ended plunger through the various optics and vacuum windows to the initial laser power, using the same power meter in both cases to remove systematic effects. The quantum efficiency of the photocathode is specified to be 40% while the collection efficiency of the metal package PMT is believed to be near 100%. The PMT pulses are amplified by 46 dB and then sent into a NIM discriminator. Using a highly attenuated LED flasher as a single photon source, the discriminator threshold is optimized to give 99.4% efficiency for triggering on single photo-electron (spe) pulses while also efficiently rejecting the sub-spe noise sources. With this threshold, and using the built-in cooler to cool the tube to 0° C, a typical measured dark count rate of $\sim$ 130 Hz is observed. The total photon counting efficiency is estimated to be $33 \pm 3.3\%$.

For timing coincidence measurements, we use modified Quarknet boards[16,17] for both laser box and PMT box signal read out. The Quarknet boards determines the time of rising and falling edges of time-over-threshold triggers from the PMT and from a monitoring photodiode that is located inside the laser box. The boards provide 1.25 ns timing precision. The clocks on the laser board and on the PMT board are synchronized using an external trigger from a signal generator. The absolute timing between the laser

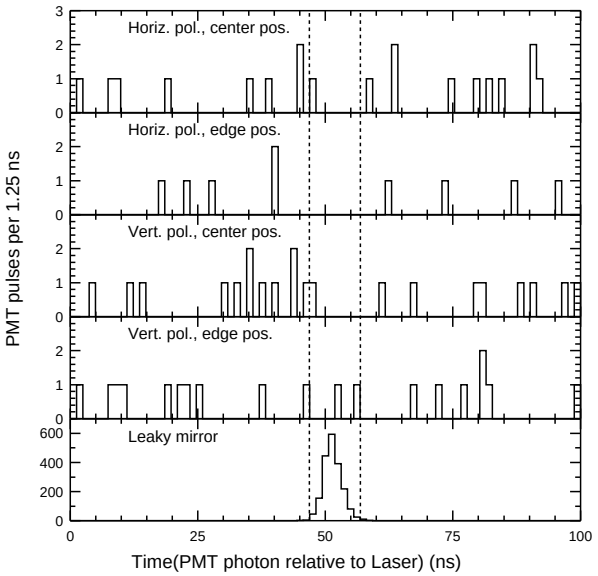

Fig. 2. PMT trigger times for the four run configurations, shown relative to the expected time distribution of photons as calibrated from the leaky mirror data.

pulses and the PMT traces is established by removing the plunger with the beam dump mirror, and allowing the laser to shine on the PMT through several attenuation stages consisting of two partially reflective mirrors, a pinhole, and multiple absorptive filters mounted directly on the aperture of the PMT module. The 10^{19} photons per second emitted by the laser are attenuated to a corresponding PMT trigger rate of less than 0.1 Hz for this timing calibration and to provide an in situ test of the data acquisition system.

For coincidence counting between the laser pulses and the PMT, a 10 ns gate is chosen to include 95% of the measured photon time distribution shown in Fig. 2. The coincident dark count rate is then estimated to be $R_{noise} = 20$ Hz$\times$120 Hz$\times$10 ns $= 2.4\times10^{-5}$ Hz. This noise rate is negligible to the expected signal rate of $\sim 2 \times 10^{-3}$ Hz estimated from the central values of the PVLAS parameters.

3. Data collection

In order to probe the entire PVLAS range of m_ϕ and g, we took four configurations of plunger position and polarization. The plunger is placed either in the center of the magnet with $L_1 = 3.1$ m and $L_2 = 2.9$ m or

near the far edge of the magnet with $L_1 = 5.0$ m and $L_2 = 1.0$ m. For each plunger position, vertically and horizontally polarized laser light is sent to into the magnet in order to test pseudoscalar and scalar couplings. The central plunger position covers most of the PVLAS signal region. Moving the plunger to the far position simultaneously changes the baseline for both the initial oscillation and the regeneration, and shifts the two regions of diminished sensitivity away. The two plunger positions thus cover the entire PVLAS signal region.

The operating conditions are monitored during each run. The reflected beam from the plunger mirror is directed into a calorimetric power meter in the laser box. The number of incident photons is determined with 10% accuracy. The beam spot is monitored using a camera which takes 30 Hz of images of the reflected laser spot on the pick-off mirror. The total pathlength to the pick-off mirror is comparable to the pathlength to the PMT; so transverse deviations seen in the images are closely matched to the deviations at the PMT. ∼mm scale transverse deviations of beam offsets are seen during the course of run due to small changes in the orientation of the plunger mirror as the plunger slowly cools through heat leaks in the warm bore insulation. In addition, the focusing lens at the PMT makes the final light collection system insensitive to these potential sub-mrad angular deviations. Nevertheless, the alignment is double-checked using the open-ended plunger after collecting data in each configuration, and no misalignment has ever exceeded our tolerances. An LED flasher fires every 5 minutes to confirm the integrity of the light collection system. The operation of the PMT is monitored using its dark rate.

4. Results

The 10 ns coincidence time window is defined using the leaky mirror data. The background in the signal region is estimated by measuring the dark count rate outside of the coincidence window. We observe no statistically significant excess above the background in any of the four configurations. Table 1 shows summary of the results. The PMT timing data, along with the leaky-mirror calibration data, are shown in an expanded time scale in Fig. 2.

The Rolke-Lopez method[18] is used to obtain limits on the regeneration probabilities, and use Eqn. 4 to obtain the corresponding 3σ upper bounds on the coupling g as a function of m_ϕ. The laser power measurement and the photon transport/detection efficiency each contribute 10% systematic uncertainty which is incorporated in the limits. These limit plots are shown

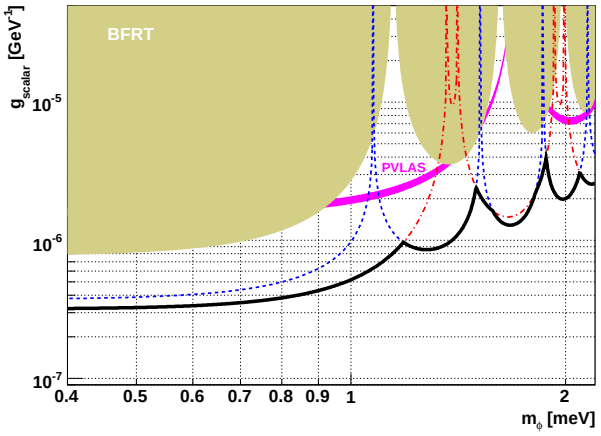

Fig. 3. 3σ limit contours for scalar particles. The solid black line is the union of the exclusion limits from the central (red dot-dashed) and the edge (blue dashed) plunger positions. The 3σ PVLAS rotation signal (pink/dark grey) and the 3σ BFRT regeneration limit (tan/light grey) are also shown.

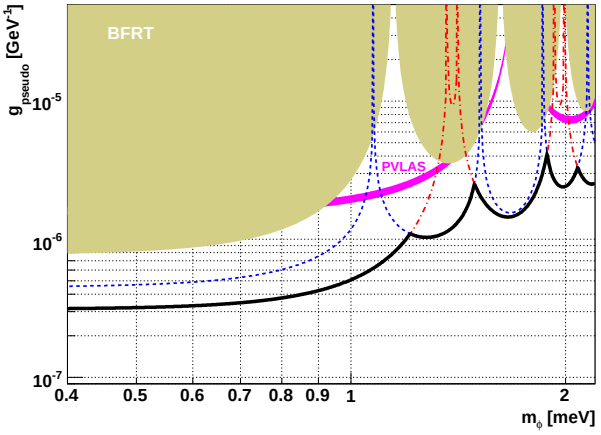

Fig. 4. 3σ limit contours for pseudoscalar particles.

in Figs. 3 and 4 along with the PVLAS 3σ signal region and the BFRT 3σ regeneration limits. As expected, the regions of insensitivity for one plunger position are well-covered by using the other plunger position. The weakly-interacting axion-like particle interpretation of the PVLAS data is excluded at more than 5σ by GammeV data for both scalar and pseudoscalar par-

Table 1. Summary of data in each of the 4 configurations.

Configuration	# photons	Est.Bkgd	Candidates	g[GeV^{-1}]
Horiz.,center	6.3×10^{23}	1.6	1	3.2×10^{-7}
Horiz.,edge	6.4×10^{23}	1.7	0	3.7×10^{-7}
Vert.,center	6.6×10^{23}	1.6	1	3.2×10^{-7}
Vert.,edge	7.1×10^{23}	1.5	2	4.5×10^{-7}

ticles. The asymptotic 3σ upper bounds on g for small m_ϕ are listed in Tab. 1. The GammeV exclusion region extends slightly beyond the previous best limit set by BFRT and sets limits in regions where BFRT had reduced sensitivity.

Acknowledgements: We would like to thank the staff of the Fermilab magnet test facility for their tireless efforts, and the technical staff of the Fermilab Particle Physics Division design group who aided in the design and construction of the apparatus. This work is supported by the U.S. Department of Energy under contract No. DE-AC02-07CH11359. AC is also supported by NSF-PHY-0401232.

References

1. R. D. Peccei and H. R. Quinn, Phys. Rev. Lett. **38**, 1440 (1977).
2. J. E. Kim, Phys. Rep. **150**, 1 (1987).
3. S. J. Asztalos, Astrophys. J. Lett. **571**, L27 (2002).
4. S. J. Asztalos, Phys. Rev. **D69**, 011101(R) (2004).
5. A. Burrows, M. T. Russel and M. S. Turner, Phys. Rev. **D42** 3297 (1990).
6. J. Engel, D. Seckel and A. C. Hayes, Phys. Rev. Lett. **65** 960 (1990).
7. E. Zavattini *et al.* [PVLAS Collaboration], Phys. Rev. Lett. **96**, 110406 (2006).
8. U. Gastaldi *et al.* [PVLAS Collaboration], Proc. XXXIII Int. Conf. on High Energy Physics, Moscow, Russia (2006).
9. R. Cameron *et al.*, Phys. Rev. D **47**, 3707 (1993).
10. G. Ruoso *et al.*, Z. Phys. C **56**, 505 (1992).
11. E. Zavattini *et al.* [PVLAS Collaboration], arXiv:0706.3419 [hep-ex].
12. C. Robilliard, R. Battesti, M. Fouche, J. Mauchain, A. M. Sautivet, F. Amiranoff and C. Rizzo, arXiv:0707.1296 [hep-ex].
13. K. Van Bibber, N. R. Dagdeviren, S. E. Koonin, A. Kerman and H. N. Nelson, Phys. Rev. Lett. **59**, 759 (1987).
14. G. Raffelt and L. Stodolsky, Phys. Rev. D **37**, 1237 (1988).
15. K. van Bibber, P. M. McIntyre, D. E. Morris and G. G. Raffelt, Phys. Rev. D **39**, 2089 (1989).
16. S. Hansen et.al, IEEE Trans.Nucl.Sci., vol. 51, no. 3, pp. 926-930 (2004).
17. H. G. Berns, et.al, IEEE Trans.Nucl.Sci., vol. 2, pp. 789-792 (2003).
18. W. A. Rolke and A. M. Lopez, Nucl. Instrum. Meth. A **458**, 745 (2001).